Mol Breeding (2022) 42: 54
https://doi.org/10.1007/s11032-022-01322-8

BnaNTT2 regulates ATP homeostasis in plastid to sustain lipid metabolism and plant growth in *Brassica napus*

Hui Xia · Yue Hong · Xiao Li · Ruyi Fan · Qing Li · Zhewen Ouyang · Xuan Yao · Shaoping Lu · Liang Guo · Shan Tang

Received: 27 July 2022 / Accepted: 15 August 2022 / Published online: 31 August 2022

Abstract The plastid inner envelope membrane-bond nucleotide triphosphate transporter (NTT) transports cytosolic adenosine triphosphate (ATP) into plastid, which is necessary for the biochemical activities in plastid. We identified a chloroplast-localized BnaC08.NTT2 and obtained the overexpressed lines of *BnaC08.NTT2* and CRISPR/Cas9 edited double mutant lines of *BnaC08.NTT2* and *BnaA08.NTT2* in *B. napus*. Further studies certified that overexpression (OE) of *BnaC08.NTT2* could help transport ATP into chloroplast and exchange adenosine diphosphate (ADP) and this process was inhibited in *BnaNTT2* mutants. Additional results showed that the thylakoid was abnormal in *a8 c8* double mutants, which also had lower photosynthetic efficiency, leading to retarded plant growth. The *BnaC08.NTT2* OE plants had higher photosynthetic efficiency and better growth compared to WT. OE of *BnaC08.NTT2* could improve carbon flowing into protein and oil synthesis from glycolysis both in leaves and seeds. Lipid profile analysis showed that the contents of main chloroplast membrane lipids, including monogalactosyldiacylglycerol (MGDG), digalactosyldiacylglycerol (DGDG), and phosphatidylglycerol (PG), were significantly reduced in mutants, while there were no differences in OE lines compared to WT. These results suggest that BnaNTT2 is involved in the regulation of ATP/ADP homeostasis in plastid to impact plant growth and seed oil accumulation in *B. napus*.

Keywords Nucleotide triphosphate transporter · Plastid · Membrane lipid · Plant growth · Oil accumulation · *Brassica napus*

Hui Xia and Yue Hong contributed equally to this work.

Supplementary Information The online version contains supplementary material available at https://doi.org/10.1007/s11032-022-01322-8.

H. Xia · Y. Hong · X. Li · R. Fan · Q. Li · Z. Ouyang · X. Yao · S. Lu · L. Guo · S. Tang (✉)
National Key Laboratory of Crop Genetic Improvement, Huazhong Agricultural University, Wuhan 430070, China
e-mail: tangshan@mail.hzau.edu.cn

H. Xia · Y. Hong · R. Fan · Q. Li · Z. Ouyang · X. Yao · S. Lu · L. Guo · S. Tang
Hubei Hongshan Laboratory, Wuhan 430070, China

X. Li
Shanghai Center for Plant Stress Biology, CAS Center for Excellence in Molecular Plant Sciences, Chinese Academy of Sciences, Shanghai 200032, China

Introduction

Plastids are semi-autonomous or involuntary plant organelles that need import some metabolites (like adenosine triphosphate (ATP), adenosine diphosphate (ADP), phosphoenolpyruvate (PEP), and pyruvate) from cytoplasm to generate organic molecules to maintain its function (Kusumi et al. 2004; Moreira et al. 2000; Mullet 1993). The plastid

membrane is composed by two membrane bilayers, and the organic molecules are easy to pass through the outer membrane, whereas difficult to pass through the inner membrane despite the help of inner membrane-bond transporters (Lyu et al. 2017; Weber 2004). ATP is supplied to plastids as extensive energy and involved in many cellular biological processes including cell growth, apoptosis, defense, and cell cycle (Reiser et al. 2004). ATP is mainly generated in mitochondria via oxidative phosphorylation, or in cytoplasm via glycolytic pathway in green tissues (Hattori et al. 2012; Flugge et al. 2011; Roux and Steinebrunner 2007; Song et al. 2006; Tang et al. 2003; Geigenberger et al. 2001). However, ATP could not cross the two-layer membranes freely (Reiser et al. 2004). Thus, membrane-bond transporters are needed to help ATP transport from cytoplasm into the plastid.

In plants, two types of ATP/ADP transporters have been reported (Rieder and Neuhaus 2011; Steinebrunner et al. 2003). One is ATP/ADP carrier in the inner mitochondria membrane, which belongs to mitochondrial carrier family. The other is plastidic nucleotide triphosphate transporter (NTT) (Weber and Linka 2011; Flugge et al. 2011). Studies showed that NTTs are important for ATP import into developing chloroplasts during chloroplast biogenesis to support the progress of ATP-dependent anabolic reactions such as starch, fatty acid (FA), and amino acid synthesis, and also maintain the phosphate homeostasis (Flugge et al. 2011; Reiser et al. 2004; Haferkamp et al. 2002; Neuhaus and Emes 2000; Tjaden et al. 1998; Mohlmann et al. 1998; Voon and Lim 2019). In higher plants, there are 11 to 12 transmembrane domains in NTT proteins, which are not structurally similar to the mitochondria ATP/ADP transporter containing six transmembrane domains (Linka et al. 2003; Winkler and Neuhaus 1999). NTTs were divided into three classes, including nucleotide antiporters as class I, proton-driven nucleotide symporters as class II, and nicotinamide adenine dinucleotide (NAD^+)/ADP antiporters as class III. Different NTT proteins showed highly dissimilar transport modes and affinities to the substrates (Schmitz-Esser et al. 2004). NTT proteins in higher plants belong to class I exhibiting highly conserved domains and similar substrate affinity (Schmitz-Esser et al. 2004). It is suggested that the function of different NTTs in higher plant is likely to be redundant.

There are two NTT isoforms in Arabidopsis, AtNTT1 and AtNTT2. Both AtNTT1 and AtNTT2 were localized in plastid showing similar transporter properties and different expression patterns (Reiser et al. 2004; Tjaden et al. 1998; Mohlmann et al. 1998). *AtNTT2* could be expressed in most tissues while *AtNTT1* represents a sugar-induced gene mainly expressed in the stem and root (Reiser et al. 2004). Co-expression of *AtNTT1* and soybean *glucose 6-phosphate/phosphate translocator* (*GPT*) raised 9% of tuber yield and 28% of starch in potato (Andersson et al. 2018; Geigenberger et al. 2001; Tjaden et al. 1998). Recent researches indicate that *NTT1* played a vital role in plant metabolism and growth in *B. napus*. Knockout of *BnaNTT1* contributed to abnormal chloroplast and plant growth (Hong et al. 2022). Other studies revealed retarded plant growth in *ntt2* and *ntt1 ntt2* double mutants with reduced primary root and delayed chlorophyll accumulations in seedlings, while *ntt1* slightly affected plant development (Reiser et al. 2004). However, the molecular mechanism of *NTT2* impacting plant growth and chlorophyll accumulation remains to be elucidated.

The synthesis of starch is an ATP-dependent reaction catalyzed by the adenosine-5-diphosphoglucose pyrophosphorylase (AGPase) consuming adenosine-5-diphosphoglucose (ADPG) and ATP (Neuhaus and Emes 2000). Due to the import of cytosolic ATP and export of ADP and phosphorus (Pi) under the action of NTT, decreased Pi content leads to improved AGPase activity which promotes starch synthesis in the plastid stroma in Arabidopsis (Neuhaus and Maass 1996; Neuhaus and Emes 2000). Moreover, FA de novo synthesis occurs in plastids or chloroplasts in higher plants (Li-Beisson et al. 2013). Subsequently, the FA is transported to different organelles to synthesize glycerolipids (Li-Beisson et al. 2013). Commonly, most of the FAs are stored in triacylglycerol (TAG) which is assembled in endoplasmic reticulum (ER) (Li-Beisson et al. 2013). TAG accumulation is regulated by many factors, such as transcription factors, oil body proteins, and FA and metabolite transporters (Li-Beisson et al. 2013). Some evidences showed that exogenous ATP could promote FA synthesis in purified plastids (Lee et al. 2017; Li et al. 2015; Cai et al. 2015; Baud et al. 2007; Qi et al. 1994; Möhlmann and Neuhaus 1994; Fan and Rawsthorne 1994; Slabas and Fawcett 1992). Abundant sugar could repress sucrose non-fermenting

1-related protein kinase1 (SnRK1) to stabilize *Wrinkled1* (*WRI1*), which plays a "push" role in FA synthesis (Vanhercke et al. 2013). In addition, the FA de novo biosynthesis begins at the acetyl-CoA catalysis by acetyl-CoA carboxylase (ACCase). ATP is needed to take part in this process (Li-Beisson et al. 2013). Similarly, the process of FA transportation from plastids to ER also needs the help of ATP (Li-Beisson et al. 2013). A study showed that OE of *glyceradehyde-3-phosphatedehydr-ogenase* (*GAPC*) significantly improved the seed oil content in Arabidopsis, while loss of *GAPC* resulted in decreased seed oil content. Meanwhile, the content of ATP was higher in OE plants and lower in mutant lines compared to WT (Guo et al. 2014).

Here, we identified four homologous genes of *NTT2* in oil crop *B. napus*. Two genes, *BnaC08.NTT2* and *BnaA08.NTT2*, showing similar and high expression levels in multiple tissues investigated in *B. napus* Transcriptome Information Resource (http://yanglab.hzau.edu.cn/BnTIR). It suggests that *BnaC08.NTT2* and *BnaA08.NTT2* may play major roles among four homologous genes because of much higher expression level in multiple tissues. We measured the ATP/ADP transport activity, metabolites and seed oil content in *BnaC08.NTT2* OE and double mutant lines. The genetic, biochemical, and metabolomic evidences indicate that *BnaNTT2* modulates the homeostasis of ATP/ADP in plastid to impact the carbon metabolism and plant growth of *B. napus*. These results demonstrate that *BnaNTT2* significantly influences the ATP/ADP homeostasis, glycolytic metabolism, starch, and FA synthesis. Elevated ATP level by *BnaNTT2* in plastid fuels seed oil accumulation which is agronomically and industrially important.

Materials and methods

Plant materials and growth conditions

Seeds from *B. napus* cultivar (cv.) Westar were germinated in pots with soil or water. One-week-old seedlings were transferred to pots and grown with regular watering of Hoaglands' nutrition solution at 25 ℃, in the greenhouse, or in field conditions from late autumn to the spring in Wuhan, China. The temperature was approximately 15–20 ℃ (day)/7–10 ℃ (night) in late autumn and 7–12 ℃ (day)/0–5 ℃ (night) in winter. For field experiment, confirmed homozygous T3 OE and mutant plants were grown in the experimental farm specific for transgenic plants. Plants were grown by a randomized plot design with three replications and each plot was about 1.6 × 1.5 m. Each line was planted in one row with 10–12 plants and plants were managed with standard field practice. Plants were harvested at mature stage and yield-related traits were measured as described previously (Lu et al. 2013).

Sequence alignment and expression analysis

Amino acid sequences in this research can be found in the GenBank (http://www.ncbi.nlm.nih.gov) and *Brassica napus* Genome Resources (http://www.genoscope.cns.fr/brass-icanapus) under the following accession numbers: NP_173003.1 for AtNTT2, XP_013587434.1 for BoNTT2, XP_009148947.1 for BrNTT2, XP_010497204.1 for CsNTT2, BnaA06g10210D for BnaA06.NTT2, BnaC05g11870D for BnaC05.NTT2, BnaA08g23810D for BnaA08.NTT2, and BnaC08g16710D for BnaC08.NTT2. Sequence alignment of AtNTT2, BoNTT2, BrNTT2, CsNTT2, and BnaNTT2 was operated using MEGA7. Expression data of *BnaNTT2* in different tissues was obtained through the *Brassica napus* Genome Resources (http://www.genoscope.cns.fr/brassicanapus).

Vector construction and plant transformation

The CDS fragment encoding the amino acids of *BnaC08.NTT2* was amplified from seedling leaves of cv. Westar. The amplified fragment was linked to the expression vector p35S-FAST driven by *Pro35S*. CRISPR-P (http://www.cbi.hzau.edu.cn/cgi-bin/CRISPR) was used to design sgRNAs. The genomic DNA sequences of *BnaC08.NTT2* and *BnaA08.NTT2* were used to predict proper target sites which could be edited by CRISPR/Cas9 system. Two sgRNAs which both targeted to *BnaC08.NTT2* and *BnaA08.NTT2* were chosen and synthesized, and cloned into the pKSE401 (Tang et al. 2018). The recombinant vectors were confirmed by PCR and sequencing. Then, they were transferred into *Agrobacterium tumefaciens* strain GV3101, respectively. The hypocotyls of Westar were infected by GV3101, and the transformation followed the method described previously

(Dai et al. 2020). In brief, seeds of cultivar Westar were immersed with 75% ethanol for 1 min, and seeds were sterilized with 0.15% (w/v) $HgCl_2$ containing 0.1% (v/v) Tween-20 for 15 min. After sterilization, the seeds were rinsed 4–5 times with sterile water. Seeds were germinated in sterilized petri dishes containing 1/2 MS solid medium and germinated in dark for 7 days at 23 °C. The hypocotyls were cut into a length of 6–8 mm for infection with *Agrobacterium* GV3101 diluted with MS medium (pH 5.8) containing 3% sucrose and 100 mM acetosyringone (AS). The infected hypocotyls were dried with sterilized filter paper and placed on a solid MS medium (pH 6.0) containing 3% sucrose, 1.8% mannitol, 1 mg L^{-1} 2,4-dichlorophenoxyacetic acid (2,4-D), 0.3 mg L^{-1} kinetin, 100 mM AS, and 3 g L^{-1} phyta-gel, for 2 days in the dark at room temperature. The hypocotyls were used to produce callus in the same medium containing 30 mM silver thiosulfate, 300 mg L^{-1} timentin, and 25 mg L^{-1} kanamycin in 8 h night/16 h day at 23 °C for 2–3 weeks. The shoots were generated from kanamycin resistant callus grown in MS (pH 6.0) containing 1% glucose, 0.25 g L^{-1} xylose, 0.6 g L^{-1} MES, 2 mg L^{-1} trans-zeatin, 0.1 mg L^{-1} IAA, 300 mg L^{-1} timentin, and 25 mg L^{-1} kanamycin for 4–6 weeks. The kanamycin-resist shoots were transferred to MS solid medium (pH 6.0) with 1% sucrose and 300 mg L^{-1} timentin for rooting. The OE plants were verified by PCR using a p35S-FAST vector specific primer and a *BnaC08.NTT2* specific primer, and the mutants were confirmed by sequencing the PCR products which were amplified using the genome DNA as the template. Primers used for the vector construction and identification of transformants are listed in Table S1.

Quantitative real-time PCR

Total RNA was isolated from leaf and seed of Westar using Transzol reagent (TransGen Biotech, Beijing, China). RNA extracts were treated with DNase I to remove gDNA and used to synthesize the first-strand cDNA by reverse transcription using a TransScript cDNA Synthesis SuperMix Kit (TransGen Biotech, Beijing, China). β*-actin* in *B. napus* was used as an internal standard (Zhou et al. 2012). Quantitative real-time PCR was performed with a MyIQ real-time PCR system (Bio-Rad, USA) using the TransStart Tip Green SuperMix (TransGen Biotech, Beijing, China). Quantitative real-time PCR conditions were set as follows: 95 □ for 30 s, 60 □ for 30 s, and 72 □ for 30 s, for 55 cycles. The primers used in quantitative real-time PCR are listed in Table S1.

Western-blot

Total protein was extracted from 1 g of leaves of OE lines and WT using buffer A containing 50 mM Tris–HCl 7.5, 10 mM KCl, 1 mM EDTA, 0.5 mM phenylmethanesulfonyl fluoride (PMSF), 2 mM dithiothreitol (DTT), and protease inhibitors (Thermo Scientific, catalog number PF200523). Fifty micrograms of protein was separated by 10% SDS-PAGE gel and the protein was transferred to PVDF membrane. The membrane was immunoblotted with anti-Flag antibody (Sigma, catalog number A3687).

Subcellular localization

The coding region of *BnaC08.NTT2* was amplified by PCR and cloned into the pMDC83 vector which contains a *GFP* gene behind the multiple clone site. The primers used are listed in Table S1. The recombinant vector was transformed into *Agrobacterium* strain GV3101 in infiltration medium (50 mM MES, 2 mM Na_3PO_4, 1 mM AS, and 5 mg mL^{-1} glucose) and co-injected into tobacco leaves with P19 for transient expression. BnaC08.NTT2-GFP fusion protein in epidermal cells was examined using confocal laser scanning microscopy (FV1200, Olympus, Japan).

Lipid extraction and analysis

About 0.1 g of leaves collected from 5-week-old seedlings grown in greenhouse was immediately immersed in 6 mL pre-heated isopropanol containing 0.02% butylated hydroxyl toluene (BHT, w/v) at 75 ℃ for 15 min. After being cooled to room temperature, 3 mL of chloroform and 1.2 mL of ddH_2O were added and incubated for 1 h by shaking. The extracts were transferred to clean glass tubes, and the remaining samples were added 4 mL of chloroform/methanol (2:1) with 0.01% BHT and shaken for 30 min. The extracts were transferred and re-extracted 3–4 times until the leaves turned white. The extracts were combined and dried under a nitrogen gas stream, and then dissolved in a certain volume of chloroform to 2 mg mL^{-1}. Lipids were

quantitatively profiled by liquid chromatography with tandem mass spectrometry (LC–MS/MS) (Lu et al. 2019; Welti et al. 2002).

Analysis of seed FA species

FA species of mature seeds and leaves were quantified using a gas chromatography-flame ionization detector (GC-FID) (QP2010 Ultra, Shimadazu, Japan) with a chromatographic RESTEK Rtx®-Wax column. The FAs were extracted and methyl-esterified as described previously (Lu et al. 2013). Finally, 1μL FA methyl ester solution from each sample was injected into the detector. The instrument parameters were set as follows: the injection port temperature was 230 ℃, and the oven temperature began at 170 ℃ for 1 min, increased by 3 ℃ min^{-1} and up to 230 ℃ for 3 min. The temperature of ion source was 200 ℃. Heptadecanoic acid (17:0, Avanti, USA) was added as an internal standard and FA species were quantified based on internal standard analysis.

Measurements of chlorophylls and their precursors

Fresh leaves (about 0.2 g) collected from 5-week-old seedlings grown in greenhouse were cut into pieces and added into 20 mL 95% ethanol. The extracts were collected to 25 mL until the leaves turned white. The absorbance values of the extracts were measured at 665, 649, and 470 nm, respectively. The contents of chlorophyll a (Chla), chlorophyll b (Chlb), and carotenoid (Car) were calculated using these equations: $Chla = 13.95 \times A_{665} - 6.88 \times A_{649}$; $Chlb = 24.96 \times A_{649} - 7.32 \times A_{665}$; $Car = (1000 \times A_{470} - 2.05 \times Chla - 114.8 \times Chlb)/245$ (Hong et al. 2018).

Fresh leaves (about 0.2 g) were collected and ground in 5 mL of extraction buffer (80% acetone), diluted to 10 mL, and then centrifuged at 12,000 g for 10 min. The absorbance values of the supernatants were measured at 575, 590, and 628 nm, respectively. The contents of protoporphyrin IX (Proto-IX), Mg-protoporphyrin IX (Mg-Proto-IX), and proto-chlorophyllide (Pchl) were calculated using these equations: $Proto\text{-}IX = (0.18016 \times A_{575}) - (0.04036 \times A_{590})$; $Mg\text{-}Proto\text{-}IX = (0.06077 \times A_{590}) - (0.01937 \times A_{575}) - (0.003423 \times A_{628})$; $Pchl = (0.03563 \times A_{628}) + (0.007225 \times A_{590}) - (0.02955 \times A_{575})$ (Hong et al. 2018).

Measurements of soluble sugar and starch content

Soluble sugar and starch contents were measured with a phenol sulfuric acid method (Chow and Landhausser 2004). For soluble sugar measurements, the small pieces of leaves or seeds were added to 25 mL ddH_2O and incubated at 95 ℃ for 30 min to release soluble sugar. The extract (50 μL) was mixed with 450 μL of sulfuric acid containing anthrone (2 mg mL^{-1}) at 95 ℃ for 5 min, and the absorbance at 625 nm was measured spectrometrically (Tecan, Infinite M200 PRD, Switzerland). The remaining sediments were desiccated at 100 ℃ overnight and homogenized with 0.2 M KOH. The homogenate was incubated at 95 ℃ for 30 min, and then mixed with 1 M acetic acid for centrifugation at 13,400 g for 5 min. The extract was measured for starch content using a method similar to that used for the determination of soluble sugar (Hong et al. 2018).

Photosynthetic efficiency measurement

The photosynthetic efficiencies, including transpiration rate, photosynthetic rate, intercellular CO_2 concentration, and stomatal conductance, were measured using photosynthetic rate meter (HED-GH20, Shandong, China). In brief, leaves from plants grew in the greenhouse were delivered to the machine, at noon. And the numbers of transpiration rate, photosynthetic rate, intercellular CO_2 concentration, and stomatal conductance for each OE and mutant lines were measured and recorded.

Chloroplast isolation

Fresh leaves (about 0.2 g) collected from 5-week-old seedlings grown in greenhouse were ground in 10 mL of pre-cooled extraction lysis buffer containing 300 mM sorbitol, 50 mM Tris pH 8.0, 5 mM EDTA pH 8.0, and 0.1%-mercaptoethanol, and then centrifuged at 700 g and 4 ℃ for 10 min. The supernatant was transferred to another tube and centrifuged at 2000 g and 4 ℃ for 10 min. The pellets were suspended in 2 mL lysis buffer and transferred to the top of 6 mL sucrose gradient buffer (4 mL bottom sucrose buffer containing 52% sucrose, 50 mM Tris pH 8.8, and 25 mM EDTA pH 8.8; 2 mL overhead sucrose buffer containing 30% sucrose, 50 mM Tris pH 8.0, and 25 mM EDTA pH 8.0) carefully, then this mixture was centrifuged at

15,000 r min^{-1} at 4 ℃ for 60 min. The isolated chloroplasts were located at the interface between overhead and bottom sucrose buffer and examined by optical microscope (BX53M, Olympus, Japan).

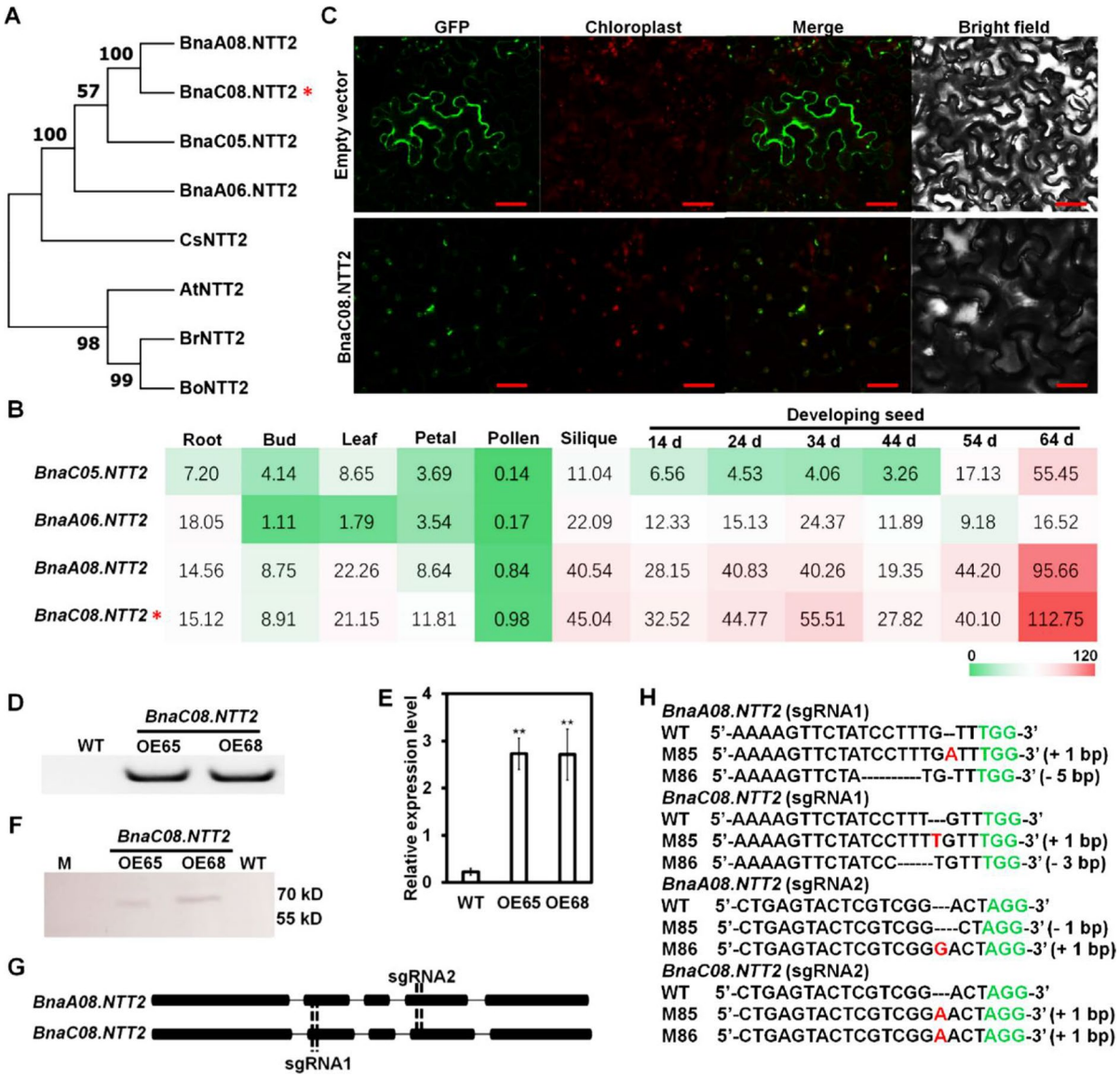

Fig. 1 Homologous gene analysis of *NTT2* and confirmation of *BnaNTT2* transgenic plants. **A** Comparison of amino acid sequence of NTT2 from different plant species using MEGA7. At, *Arabidopsis thaliana*; Bn, *B. napus*; Bo, *B. oleracea*; Br, *B. rapa*; Cs, *Camelina sativa*. **B** The expression of *NTT2s* in different tissues of *B. napus*. Gene expression data are from BnTIR (http://yanglab.hzau.edu.cn/). BnaC06.NTT2 is marked in red star in **A** and **B**. **C** BnaC08.NTT2 is localized on chloroplast membrane observed in tobacco epidermal cells under confocal microscopy. Bars = 25 μm. **D** Identification of the *BnaC08.NTT2* overexpression lines using PCR. **E** Expression level of *BnaC08.NTT2* in overexpression lines by quantitative real-time PCR. Total RNA was extracted from leaves of 5-week-old plants. β-*actin* was used as an internal standard and for normalization. Values are means ± SD ($n = 3$). **Indicates $P < 0.01$, based on a student *t*-test. **F** Detection of the *BnaC08.NTT2* expression in overexpression lines by Western-blot. **G** CRISPR target sites on *NTT2*s of *B. napus*. **H** Confirmation of *BnaC08.NTT2* and *BnaA08.NTT2* double mutants (M85 and M86) by sequencing. Insertions are indicated in red and deletions are indicated in black dotted line. PAM sites are indicated in green

Isolation of chloroplast subfractions

Fresh leaves (about 2.0 g) were collected from 5-week-old seedlings grown in the greenhouse. Chloroplasts were isolated according to the method described above. Purified chloroplasts were suspended in hypertonic medium (0.7 M mannitol, 4 mM $MgCl_2$, 1 mM PMSF, 1 mM benzamidine, 0.5 mM ε-amino caproic acid, 20 mM MOPS-NaOH, pH 7.8). Suspension was rapidly homogenized by filtration and incubated 10 min on ice before loading in a pre-cold Yeda press. Liquid was released from the press (10 mL min^{-1}) and collected on ice. The liquid was centrifuged at 12,000 g and 4 ℃ for 10 min and

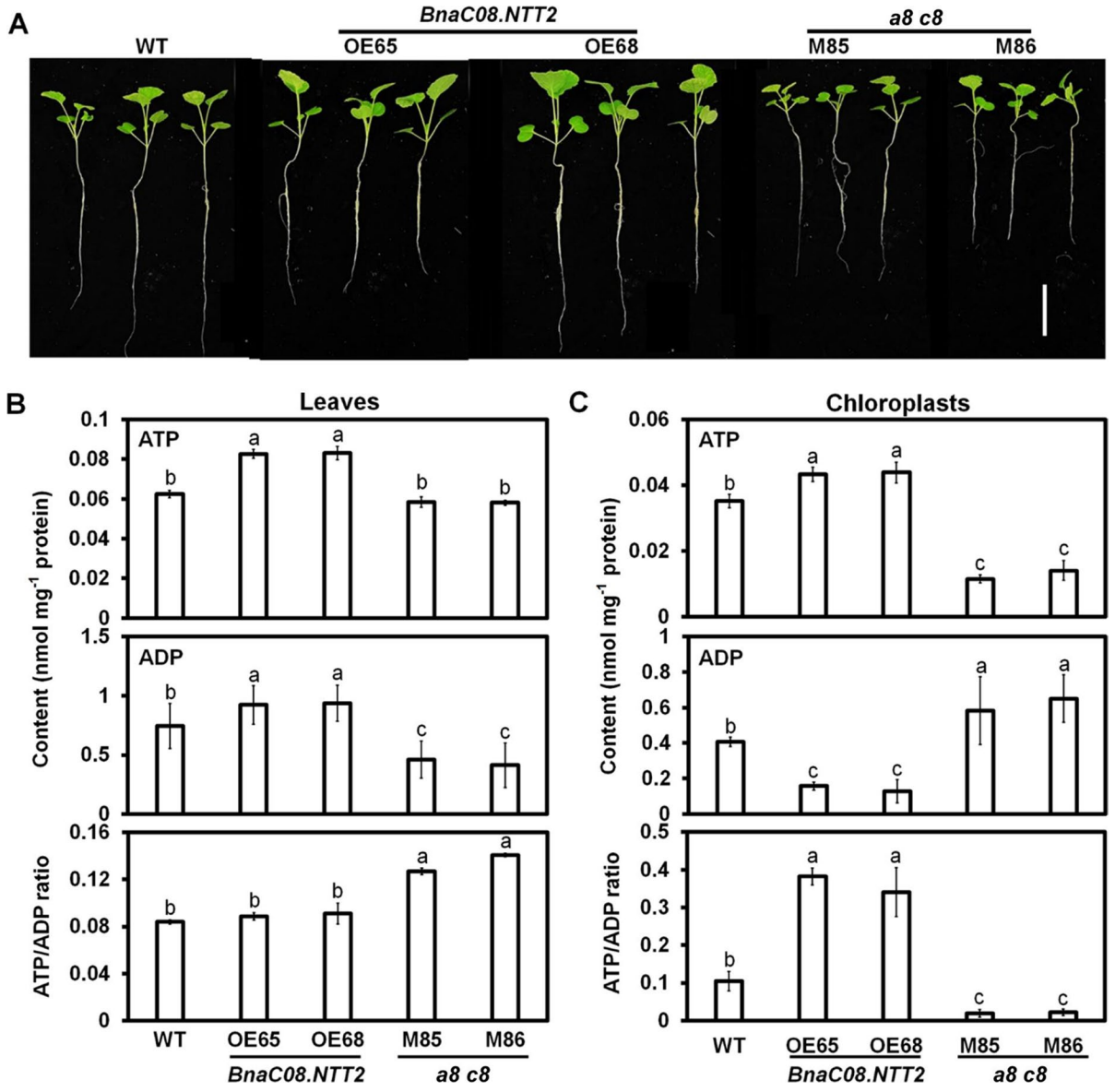

Fig. 2 Phenotype of transgenic plants and contents of ATP and ADP in leaves and chloroplasts. **A** Phenotype of *BnaNTT2* transgenic plants when they grew in liquid media for 5 weeks. Bars = 5 cm. **B** Contents of ATP and ADP in leaves. Samples were taken from 5-week-old plants. Values are means ± SD ($n = 5$). **C** Contents of ATP and ADP in chloroplasts. Chloroplasts were isolated from the leaves of 5-week-old plants. Values are means ± SD ($n = 5$). Different letters represent significant differences at $P < 0.05$, based on ANOVA analysis and Duncan's multiple-range test

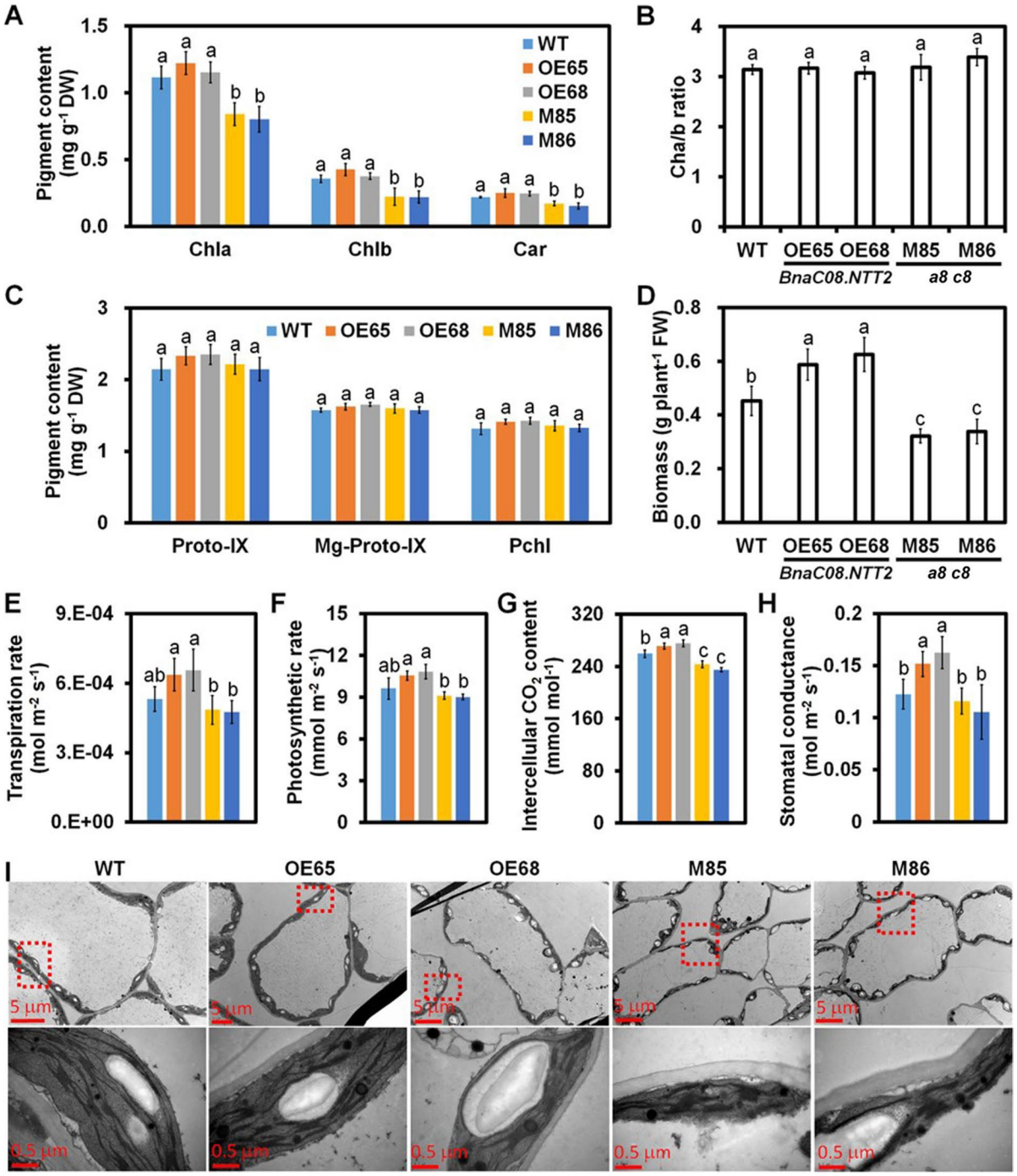

the supernatant was centrifuged twice at 12,000 g and 4 ℃ for 10 min to remove complete chloroplasts. The supernatant was loaded on top of 24 mL sucrose gradient buffer (8 mL of 1.1 M sucrose (1.1 M sucrose, 1 mM EDTA, 10 mM HEPES–KOH, pH 7.8), 8 mL of 0.65 M sucrose (0.65 M sucrose, 1 mM EDTA, 10 mM HEPES–KOH, pH 7.8), and 8 mL of 0.4 M sucrose (0.4 M sucrose, 4 mM $MgCl_2$, 1 mM PMSF, 1 mM benzamidine, 0.5 mM ε-amino caproic acid, 20 mM MOPS-NaOH, pH 7.8)) carefully and

◂**Fig. 3** Changes in plant biomass, pigment contents, and photosynthesis efficiency in transgenic plants. **A** Contents of chlorophyll a and b, and carotenoid in leaves. Samples were taken from plants shown in Fig. 2A. Values are means ± SD ($n = 3$). Chlorophyll a, Chla; Chlorophyll b, Chlb; Carotenoid, Car. **B** Chlorophyll a/b ratio in leaves. Values are means ± SD ($n = 3$). **C** Contents of chlorophyll precursors when plants were 5-week-old. Values are means ± SD ($n = 3$). Proto-IX, protoporphyrin IX; Mg-Proto-IX, Mg protoporphyrin IX; Pchl, protochlorophyllide. **D** Fresh weight of 5-week-old plants. Values are means ± SD ($n = 3$). The indexes related to leaf photosynthesis including **E** transpiration rate, **F** photosynthetic rate, **G** intercellular CO_2 concentration, and **H** stomatal conductance. Values are means ± SD ($n = 3$). Different letters represent significant differences at $P < 0.05$, based on ANOVA analysis and Duncan's multiple-range test. **I** Ultra-structure of chloroplast observed under transmission electron microscope. Samples were taken from 5-week-old plants. Pictures below are enlarged image of the picture, showed in red box with dot lines

centrifuged at 80,000 g and 4 ℃ for 90 min. The outer envelope membranes (OMs) were collected as a layer at the 0.4–0.65 M sucrose interface and the inner envelope membranes (IMs) were collected as a layer at the 1–0.65 M sucrose interface. And the thylakoids were collected at the bottom of the tubes (Block 2018). Each chloroplast subfraction was kept on ice and diluted in 2 × SDS-PAGE dying buffer (1:1, v/v). Equal amount of protein (10 μg) from purified chloroplast and each chloroplast subfraction was loaded on SDS-PAGE and the expression of BnaC08.NTT2 was examined by western-blot using Flag antibody as described above.

Metabolite analysis by LC–MS/MS

Metabolite extraction and analysis was performed according to the method described previously (Guo et al. 2014). Leaves were harvested from 5-week-old seedlings and ground in liquid nitrogen immediately. Metabolites were extracted from about 0.1 g leaf powders or chloroplasts isolated from 0.2 g leaves with 3 mL methanol-chloroform (7:3, v/v) and incubated at − 20 ℃ for 2 h with occasional vortexing. A total of 0.9 μg 1,4-piperazinediethanesulfonic acid (PIPES) was added to each sample as internal standard. Water soluble metabolites were extracted by adding 2.4 mL ddH_2O and centrifuged at 500 g for 5 min. The upper phase was removed to a new glass tube. The upper phase was dried with gas nitrogen at room temperature, re-dissolved with 200 L ddH_2O and diluted by tenfold for metabolite analysis by LC–MS/MS (QTRAP® 6500 + , AB SCIEX, USA). The level of metabolites was determined by compared to PIPES.

Microscopic observation of Brassica napus seed-coat mucilage

Seed-coat mucilage was stained by the ruthenium red followed the procedure as reported (Li et al. 2020). In brief, dry mature seeds were sunk into 0.05 M EDTA pH 8.5 for 1 h, stained in 0.01% ruthenium red (w/v) for another 1 h, and washed by ddH_2O. Observation was carried out under an optical microscope (BX53M, Olympus, Japan).

Statistical analysis

Microsoft Excel (2016) was used to calculate *P*-value by paired two-tailed Student's *t* test methods. SAS (Statistical Analysis System) was used to calculate *P*-value based on ANOVA analysis and Duncan's multiple-range test.

Results

Analysis of NTT2 homologous genes in B. napus and acquirement of transgenic plants

Through the amino acid sequence alignment of AtNTT2, there are four *BnaNTT2* genes in *B. napus* genome, designated *BnaC05.NTT2*, *BnaA06.NTT2*, *BnaA08.NTT2*, and *BnaC08.NTT2*. Four BnaNTT2s were close homologous with the AtNTT2, BoNTT2 (*B. oleracea*), BrNTT2 (*B. rapa*), and CsNTT2 (*Camelina sativa*) (Fig. 1A and Table S2). Expression levels of *BnaC08.NTT2* and *BnaA08.NTT2* are much higher than that of *BnaC05.NTT2* and *BnaA06.NTT2* in developing seeds and other tissues except root (Fig. 1B). In addition, expression of *BnaC08.NTT2* in these tissues is a little higher than that of *BnaA08.NTT2* (Fig. 1B). Sequence alignment of BnaC08.NTT2 and BnaA08.NTT2 shows that they share the similar amino acid sequence and protein structures (Fig. S1). It suggests that the function of BnaC08.NTT2 and BnaA08.NTT2 may be redundant. BnaC08.NTT2 was fused with green fluorescence protein (GFP) at its C-terminus to construct a BnaC08.NTT2-GFP vector, which was transiently

expressed in epidermal cells of tobacco leaves. The green fluorescence of BnaC08.NTT2-GFP was completely overlaid with the auto-fluorescence of the chloroplast, suggesting that BnaC08.NTT2 was localized on chloroplast membrane (Fig. 1C).

To explore the function of *BnaNTT2* in *B. napus*, transgenic lines including OE lines of *BnaC08.NTT2* and CRISPR/Cas9 edited mutants of *BnaC08.NTT2* and *BnaA08.NTT2* were obtained by *Agrobacterium*-mediated genetic transformation. Nine OE plants are obtained, and two of them (OE65 and OE68) are confirmed by PCR and chosen for further study because of higher expression level (Figs. 1D and E and S2). Furthermore, OE65 and OE68 are confirmed by Western-blot (Fig. 1F). For CRISPR/Cas9 edited mutants, two sgRNAs were designed to mutate

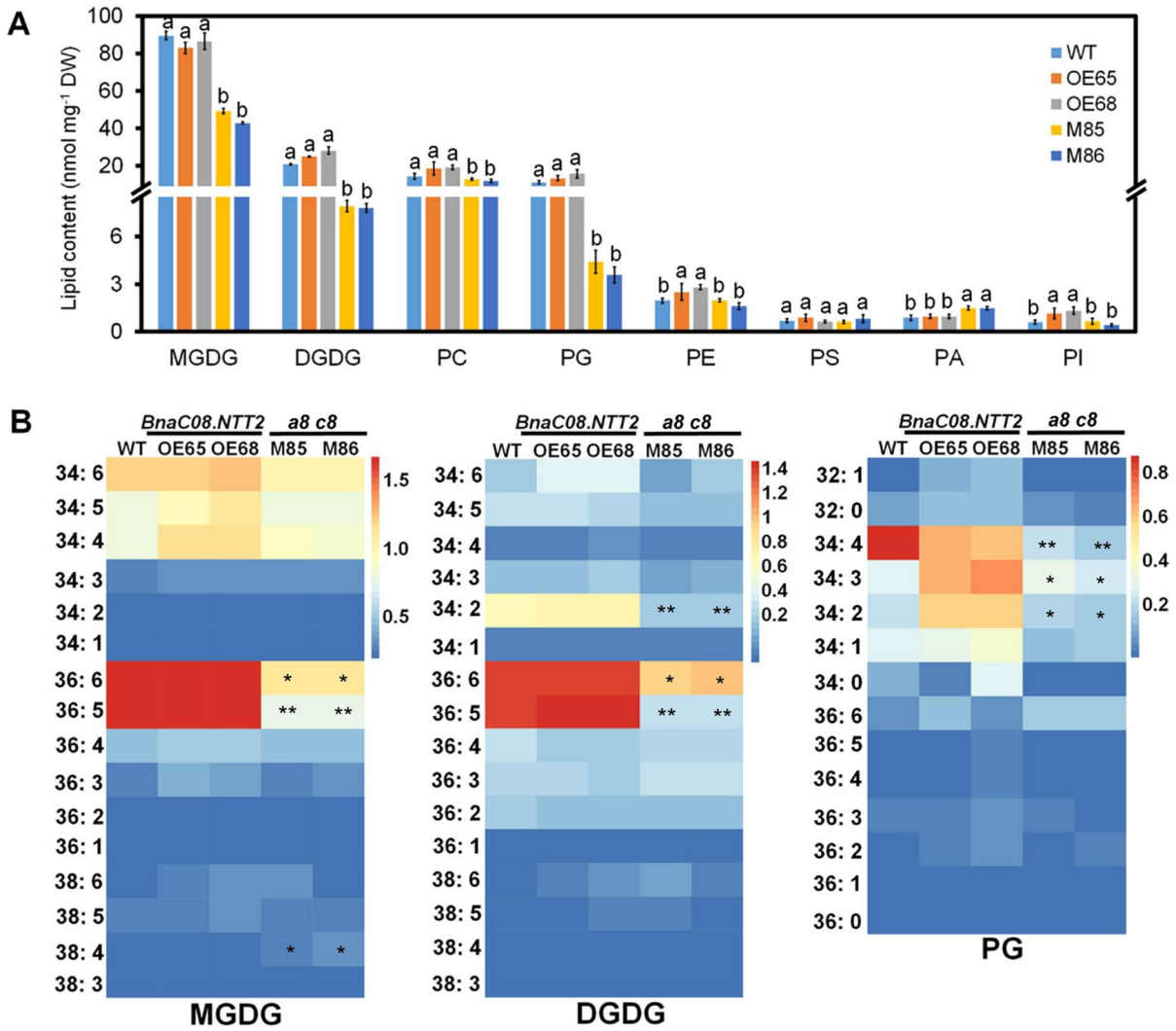

Fig. 4 Contents and compositions of lipids in transgenic and WT plant leaves. **A** Comparison of glycerolipids' contents among OE, double mutant and WT leaves. Samples were taken from 5-week-old plant leaves. Values are means ± SD ($n = 5$). Different letters represent significant differences at $P < 0.05$, based on ANOVA analysis and Duncan's multiple-range test. **B** Contents of different species of MGDG, DGDG, and PG in transgenic and WT plant leaves. Average data of each species of MGDG, DGDG, and PG were normalized by a $\log_{10}$ calculation and then the heat map was drawn using image GP online tool (www.ehbio.com/ImageGP). Each vertical colored bar represents the $\log_{10}$ of concentration (nmol mg^{-1} dry weight) as shown in the color key. *Indicates $P < 0.05$ and **indicates $P < 0.05$, based on a student *t*-test. MGDG, monogalactosyldiacyglycerol; DGDG, digalactosyldiacylglycerol; PG, phosphatidylglycerol

BnaC08.NTT2 and *BnaA08.NTT2* (Fig. 1G). Finally, two homozygotes, M85 and M86, with mutant sites both in *BnaC08.NTT2* and *BnaA08.NTT2* are chosen for further study (Fig. 1H). Furthermore, isolation of chloroplast subfractions of OE65 and WT was performed. The result of western-blot shows that BnaC08.NTT2 is localized on the inner envelope membrane (Fig. S3).

BnaNTT2 caused alteration of ATP/ADP ratio both in whole leaf and chloroplast

To investigate whether BnaNTT2 could impact plant growth, WT and transgenic lines were grown for 5 weeks. The OE plants that were observed grew better while the double mutant seedlings grew smaller with pale-yellow leaves compared to WT (Fig. 2A). Chloroplasts were isolated from the *B. napus* leaves and confirmed by optical microscope (Fig. S4). ATP and ADP levels in whole leaves and chloroplasts were measured by LC–MS/MS. In whole leaves, contents of ATP and ADP in two OE lines are increased by 32.2% and 10.6%, compared to WT, respectively (Fig. 2B). Contents of ATP in M85 and M86 show no difference with WT, but ADP contents are decreased by 57.3% (Fig. 2B). Finally, the ATP/ADP ratio is not changed in OE lines compared to WT, but significantly increased in mutants (Fig. 2B). In isolated chloroplasts, ATP levels are increased by 34.2% while ADP levels are reduced by 58.5% in two OE lines compared to WT (Fig. 2C). On the contrary, M85 and M86 display decrease of ATP levels by 60.5% and 55.2%, but increase of ADP levels by 45.2% and 62.5% compared to WT, respectively (Fig. 2C). The ATP/ADP ratios in OE and *a8 c8* mutant chloroplasts are nearly 3.8-fold and 0.3-fold to that in WT (Fig. 2C). These results indicate that BnaNTT2 could enhance ATP accumulation and decrease ADP content in plastid.

BnaNTT2 affects photosynthetic efficiency

When plants grew up to 5-week-old, pigment content was detected. Contents of Chla, Chlb, and Car in leaves have no difference between OE and WT. However, contents of Chla, Chlb, and Car are reduced by 48.1%, 55.5%, and 16.2% in *a8 c8*, respectively (Fig. 3A). It is interesting that the ratio of chlorophyll a/b is not changed among WT, OE and *a8 c8* plants (Fig. 3B). Contents of chlorophyll precursors including Proto-IX, Mg-Proto-IX, and Pchl were also measured at the same time. The results show that the levels of Proto-IX, Mg-Proto-IX, and Pchl in WT, OE, and *a8 c8* plants are nearly comparable (Fig. 3C). These results imply that the changes of Chla, Chlb, and Car are not resulted from chlorophyll synthesis. The fresh weight levels of OE65 and OE68 are increased by 22.2% and 37.7% compared to that of WT, respectively. While they are decreased by 25.8% in *a8 c8* lines (Fig. 3D).

Chloroplast is the main place for photosynthesis in plant. The photosyntheses in leaves of WT, OE, and *a8 c8* plants were detected using a photo-synthesizer. The indexes of transpiration rate and photosynthetic rate both in OE and *a8 c8* have no significant difference compared to WT while they are significant higher in OE than *a8 c8* (Fig. 3E and F). On the other hand, the levels of intercellular CO_2 concentration and stomatal conductance are higher in OE plants than that in WT. In contrast, they are lower in mutants (Fig. 3G and H). The ultrastructure of mesophyll cells from leaves was observed under transmission electron microscope (TEM). Compared to WT, *a8 c8* lines display smaller chloroplast size and impaired thylakoid structure with a smaller and irregular distribution of grana (Figs. 3I and S4). These results indicate that BnaNTT2 has important role in the regulation of chloroplast development.

BnaNTT2 changes the lipid contents in OE and double mutant leaves

Impaired thylakoid structure indicates that the membrane lipids may be altered. To analyze the lipid contents in OE and *a8 c8* plants, lipids were extracted from leaves of 5-week-old plants. LC–MS/MS was used to analyze the extracts using the method described previously. The data show that the main chloroplast membrane lipids including monogalactosyldiacylglycerol (MGDG), digalactosyldiacylglycerol (DGDG), and phosphatidylglycerol (PG) are decreased by 47.7%, 64.3%, and 69.4% in *a8 c8* leaves than those in WT, respectively (Fig. 4A). The decreased MGDG, DGDG, and PG are mainly caused by the reduced MGDG-36:5 and -36:6, DGDG-34:2, -36:5, and -36:6, PG-34:2, -34:3, and -34:4 species, respectively (Fig. 4B). However, levels of MGDG,

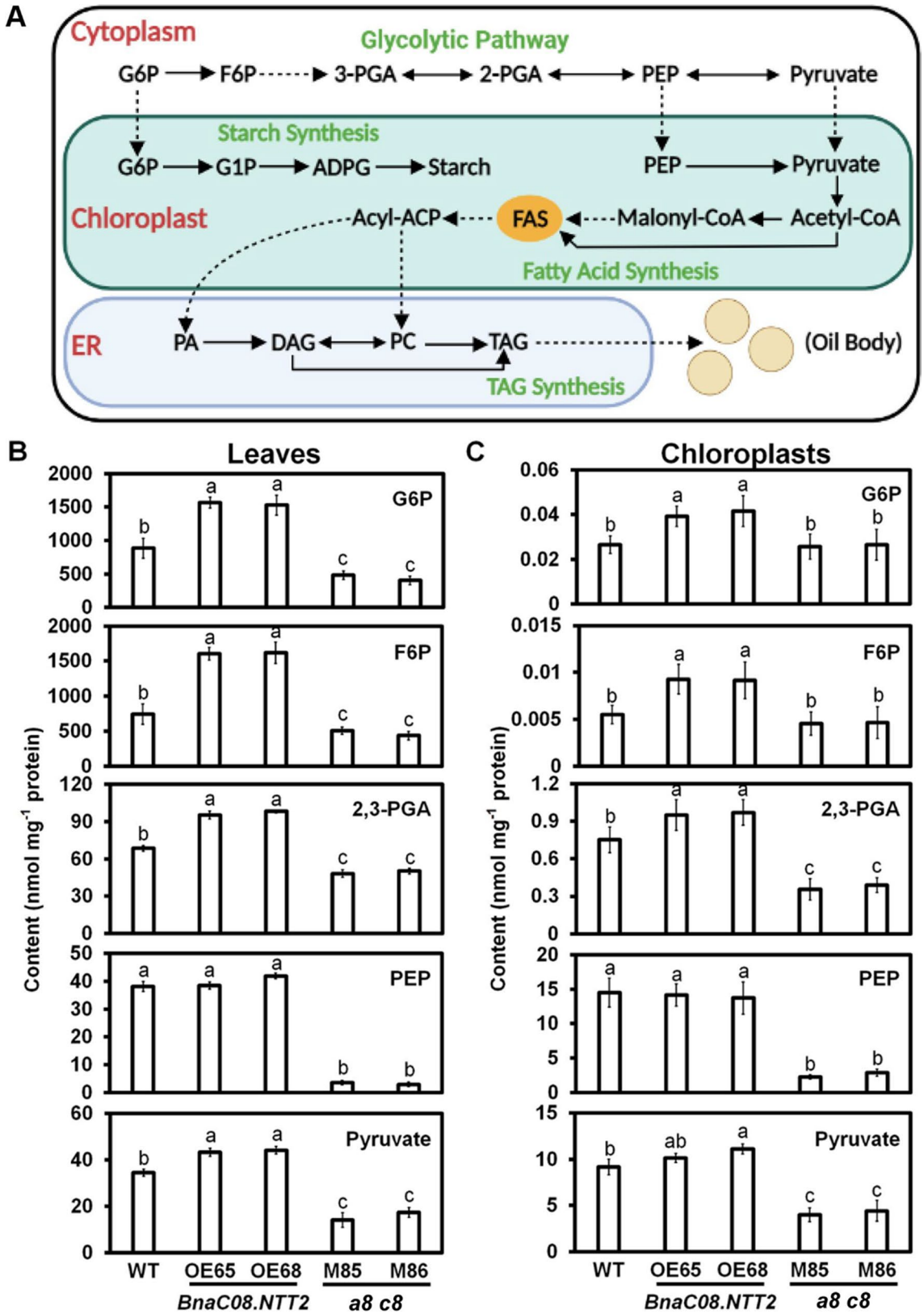
A
Cytoplasm
Glycolytic Pathway
G6P
F6P
3-PGA
2-PGA
PEP
Pyruvate
Starch Synthesis
G6P
G1P
ADPG
Starch
PEP
Pyruvate
Chloroplast
Acyl-ACP
FAS
Malonyl-CoA
Acetyl-CoA
Fatty Acid Synthesis
ER
PA
DAG
PC
TAG
(Oil Body)
TAG Synthesis
B
Leaves
C
Chloroplasts
G6P
F6P
2,3-PGA
PEP
Pyruvate
Content (nmol mg-1 protein)
WT
OE65
OE68
M85
M86
BnaC08.NTT2
a8 c8

◂**Fig. 5** BnaNTT2 accelerates the process of glycolysis in leaves and chloroplasts. **A** Brief diagram of carbon flux from glycolysis to starch and TAG synthesis in leaves. **B** Contents of some metabolites in glycolysis in leaves. Samples were taken from 5-week-old plants. Values are means ± SD ($n = 5$). **C** Contents of some metabolites in glycolysis in chloroplasts. Samples were taken from 5-week-old plants. Values are means ± SD ($n = 5$). Different letters represent significant differences at $P < 0.05$, based on ANOVA analysis and Duncan's multiple-range test. G6P, glucose-6-phosphate; 2-PGA, 2-phosphoglycerate; 3-PGA, 3-phosphoglycerate; PEP, phosphorenlpyruvate. G1P, glucose-1-phosphate; ADPG, adenosine-5-diphosphoglucose

DGDG, and PG are not changed between OE and WT (Fig. 4A). In *a8 c8* plants, phosphatidylcholine (PC) has a little reduction while phosphatidic acid (PA) has increased content in mutant lines. Phosphatideylethanolamine (PE), phosphatidylserine (PS), and phosphatidylinositol (PI) are nearly the same as WT (Fig. 4A). Besides, contents of PE and PI are increased in OE plants (Fig. 4A). These results indicate that BnaNTT2 plays an important role in modulating membrane lipids.

BnaNTT2 affects glycolysis and fatty acid synthesis in leaves

To determine the effect of BnaNTT2 on primary metabolism, chloroplasts were extracted and purified from the leaves of WT, OE, and *a8 c8* plants (Fig. S5). A simple model of carbon flux from glycolysis to starch and TAG biosynthesis is shown in Fig. 5A. The LC–MS/MS was used to detect the contents of metabolites in glycolysis including glucose-6-phosphate (G6P), PEP, and pyruvate both in whole leaves and chloroplasts. Besides, fructose-6-phosphate (F6P) and phosphoglycerate (2-PGA, 3-PGA) in leaves, in chloroplast, were detected following the previous study (Guo et al. 2014). The results show that all of them are significantly increased both in leaves and chloroplasts of OE plants than those in the WT, except PEP (Fig. 5B and C). In contrast, contents of metabolite in *a8 c8* leaves and chloroplasts are significantly decreased, except no change in the contents of G6P in chloroplasts (Fig. 5B and C). Additionally, FA contents in leaves are increased in OE plants, but no alterations in *a8 c8* leaves are observed (Fig. S6). Specifically, contents of C16:0, C18:1, and C18:3 of OE plants are 6.67%, 15.3%, and 11.8% higher than that in WT, respectively (Fig. S6). To understand how BnaNTT2 affects FA biosynthesis in leaves, expression levels of key genes involved in transcription regulation, starch synthesis, FA synthesis, TAG synthesis, and oil body formation were measured by quantitative real-time PCR. The data display that the expression levels of *WRI1*, *starch synthase1* (*SS1*), *malonyltransferase* (*MCMT*), *phosphatide phosphatase* (*PAP*), *diacylglycerol acyltransferase* (*DGAT*), *phospholipid: diacylglycerol acyltransferase* (*PDAT*), *oil body oleosin 1* (*OBO1*), and *oil body oleosin 3* (*OBO3*) in the OE plants are significantly higher than those in WT, while the expression levels of *glycerol-3-phosphate dehydrogenase* (*GPDH*) and *caleosin* (*CALO*) are much lower in OE plants (Fig. S7). Expression levels of those genes in *a8 c8* lines are significantly lower than those in WT (Fig. S7). These results imply that BnaNTT2 impacts glycolysis and controls carbon flux to influence the synthesis of FA in leaves.

BnaNTT2 improves seed oil accumulation by impacting key lipid synthesis genes

We investigated the agronomic traits of WT and transgenic mature plants grown in the field. Yields per plant of OE plants (OE65 and OE68) are significantly increased compared with WT, and mutant plants exhibit significantly decreased yield (Table S3). The main inflorescence length, number of effective branches, and effective silique number of the mutant plants are also significantly lower than those of WT and OE plants (Table S3). The results imply that *BnaC08.NTT2* is required to maintain plant growth while loss of *BnaC08.NTT2* would inhibit plant growth and seed yield in *B. napus*. Besides, expression levels of *BnaC08.NTT2* OE lines are significantly increased than the WT in seeds, indicating that *35S* promoter is active in seeds and *BnaC08.NTT2* is also overexpressed in the seeds of OE lines (Fig. S8). In order to determine the effect of BnaNTT2 on seed, several traits were compared among WT, OE, and *a8 c8* seeds. Seed sizes of *a8 c8* lines are significantly smaller than WT (decreased by around 17%), with more released seed coat mucilage. While these phenomena are not obviously observed in OE compared to WT (Fig. 6A and B). Furthermore, contents of soluble sugar and starch are not changed in OE seeds, but much lower in *a8 c8* seeds, compared to WT (Fig. 6D and E). The protein content is significantly

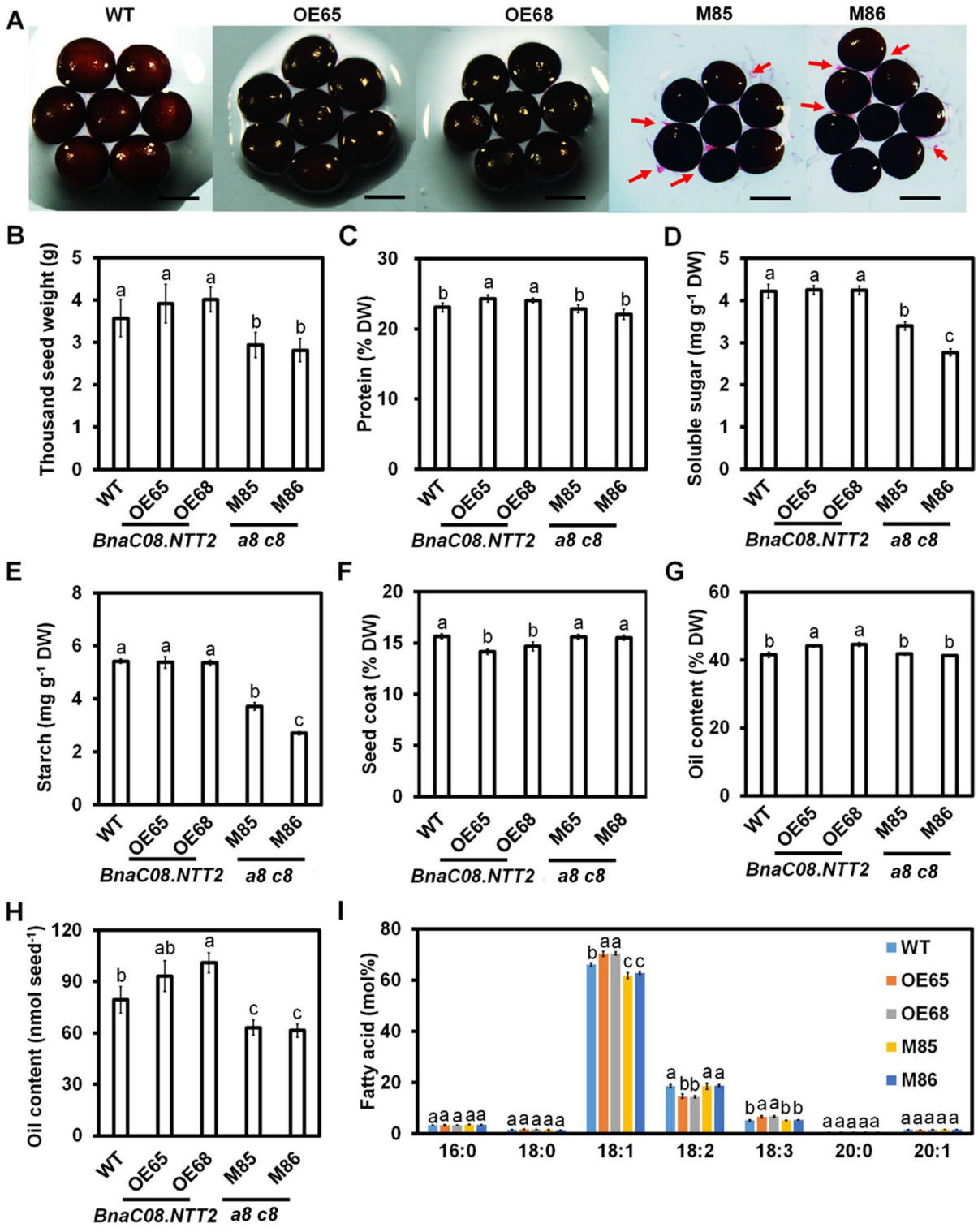

higher and the percentage of seed coat is lower in OE seeds than those in WT, respectively. However, there are no difference between *a8 c8* and WT seeds (Fig. 6C and F). Compared to WT, oil content of OE

◂**Fig. 6** BnaNTT2 promotes seed protein and oil accumulation with changed fatty acid composition. **A** Measurement of mature seed coat mucilage leakage. The red arrows indicated the seed coat mucilage leakage from mature seeds. Bars = 0.5 mm. **B** Thousand seed weight of mature seeds. Values are means ± SD ($n = 10$). **C**–**E** The contents of protein, soluble sugar, and starch in mature seeds. Values are means ± SD ($n = 5$). **F** The percentage of seed coat in measure seed. Values are means ± SD ($n = 20$). **G** Seed oil content. Values are means ± SD ($n = 5$). **H** Seed oil content per seed. Values are means ± SD ($n = 5$). **I** Fatty acid composition in seed. Values are means ± SD ($n = 5$). Different letters represent significant differences at $P < 0.05$, based on ANOVA analysis and Duncan's multiple-range test

seeds is increased by 6.1–7.8%, but not significantly changed in *a8 c8* seeds (Fig. 6G). Oil content per seed of OE lines is increased by 17.7% while decreased by 22.7% in *a8 c8* seeds (Fig. 6H). Contents of FA composition show that C18:1 and C18:3 are significantly increased in OE seeds in comparison with WT, but the content of C18:1 is decreased in *a8 c8* seeds (Fig. 6I). To understand the change of oil content in seeds from transgenic plants, expression levels of key genes involved in controlling carbon flux and oil biosynthesis were detected by quantitative real-time PCR in 35 day-after-flowering seeds. The results display that the expression levels of *SS1*, *SS2*, *MCMT*, *ENR*, *GPDH*, *PAP*, *DGAT*, *PDAT*, *OBO1*, *OBO2*, *OBO3*, and *CALO* in OE seeds are significantly higher than those in WT (Fig. S9B–S9E). Most of them have no difference between mutant seeds and WT, except *DGAT*, *PDAT*, *OBO1*, and *OBO2* (Fig. S9D–S9E). Surprisingly, the expression of *WRI1* has no difference among OE, mutant, and WT seeds (Fig. S9A). These results demonstrate that BnaNTT2 promotes oil accumulation by impacting the expression of key genes related to the starch, fatty acid, and TAG synthesis.

Discussion

NTT is responsible for transporting cytosolic ATP into plastid and exchanging ADP and Pi into cytoplasm to satisfy the needs of metabolism activities (Trentmann et al. 2008; Voon and Lim 2019). The NTT protein has been reported to be expressed in *E. coli* to transport radioactively labeled ATP (Tjaden et al. 1998). But there is no direct evidence to certify whether NTT could bind and transport cytosolic ATP into plastid in higher plants. We provided evidences that chloroplast-localized BnaC08.NTT2 could enhance ATP accumulation and decrease ADP content in plastid (Figs. 1C and 2C). The ATP contents are observed increased in OE chloroplasts and decreased in mutant chloroplasts, and the content of ADP decreased in OE and increased in *a8 c8* mutants (Fig. 2C). These biochemical evidences support that BnaNTT2 plays an important role in transporting ATP into chloroplasts. Furthermore, more elaborate experiments need to be done to directly certify that the BnaNTT2 can import cytosolic ATP into chloroplast and output plastidial ADP to cytoplasm in *B. napus*.

MGDG, DGDG, and PG are main membrane lipid component in thylakoid (Li-Beisson et al. 2013). Previous studies showed that ATP generated from the photosystem could be anchored to the thylakoid membrane in green tissues (Hattori et al. 2012; Flugge et al. 2011; Roux and Steinebrunner 2007; Song et al. 2006; Tang et al. 2003; Steinebrunner et al. 2003; Geigenberger et al. 2001). The OE plants show greater growth with higher photosynthetic rate, while the double mutants exhibit weaker growth and pale-yellow leaves with abnormal thylakoid structures (Figs. 2 and 3). Contents of MGDG, DGDG, and PG are decreased in *a8 c8* mutants compared to WT (Fig. 4). However, contents of chlorophyll precursors have no difference between WT and *a8 c8* (Fig. 3C). We speculate that BnaNTT2 plays a role in maintaining chloroplast structure but not in chlorophyll synthesis.

In seeds, glycolysis is the common carbon source for the synthesis of starch and FAs (Xu and Shanklin 2016). Previous research reported that *WRI1* is a key regulator which promotes the expression levels of genes involved in glycolysis and FA biosynthesis, and participated in plant lipid metabolism in leaves, while expression level of *WRI1* decreased in mature seed (Kong et al. 2020; Kong and Ma 2018; To et al. 2012; Bourgis et al. 2011; Maeo et al. 2009; Baud et al. 2009; Cernac and Benning 2004). OE of *WRI1* leads to increased oil content in both seeds and leaves (Reynolds et al. 2015; van Erp et al. 2014; Sanjaya et al. 2011). Besides, promoted glycolysis was reported to enhance the effect of the *WRI1* in vegetative tissues (Zhai et al. 2021; Cernac and Benning 2004). Similar phenotypes were also observed in our study. Higher lipid content in leaves in OE lines might be caused by induced expression of *WRI1*, thus upregulating the expression of key genes involved in lipid synthesis (Figs. S7 and S9).

The contents of protein and oil were both accumulated in mature seed. Decreased seed coat content of OE seeds leading to increased proportion of embryo in seeds might be the main reason for higher seed oil and protein contents, compared with the WT (Fig. 6C, F, and G). Besides, lower seed oil content in *a8 c8* might be caused by downregulation of expression of key genes involved in starch synthesis, fatty acid synthesis, TAG synthesis, and oil body formation, while another reason for lower seed oil content in *a8 c8* might be the less metabolites and ATP supplying in chloroplast resulted in reduced seed size with WT (Figs. 6 and 7). These results indicate that BnaNTT2 plays a role in regulating seed size and seed coat content through mediating the energy supply to impact seed protein and oil accumulations.

In *B. napus*, another plastid-localized NTT protein BnaNTT1 was identified. BnaNTT1 transported cytosolic ATP into plastids and functioned in modulating ATP homeostasis in plastids to sustain metabolism and growth (Hong et al. 2022). In this study, *BnaNTT2* shows similar phenotype to that of *BnaNTT1* in mutants, such as abnormal thylakoid structures, plant growth, and the levels of metabolites. Sequence alignment showed that NTT1 and NTT2 had high homology and similar conserved transmembrane domains (Reiser et al. 2004), which implied conserved function for NTT1 and NTT2. However, we found that different expression levels were exist in several tissue of *B. napus*. *BnaNTT1* showed high expression levels in the early stage of a developing seed, while *BnaNTT2* shows high expression in the late stage of a developing seed (Fig. 1B), which implies *BnaNTT1* and *BnaNTT2* may make different contributions to seed oil accumulation. How combination of *BnaNTT1* and *BnaNTT2* affects seed oil accumulation is a question worth solving.

In summary, the chloroplast-localized BnaNTT2 transports cytosolic ATP into plastid and exchanges ADP into cytoplasm in *B. napus*. FAs synthesized in

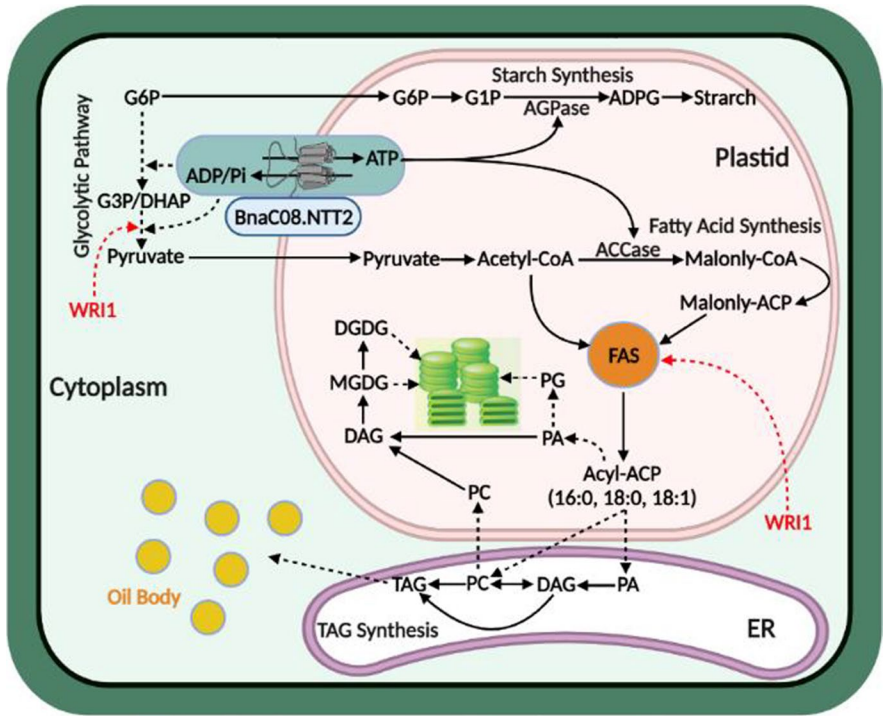

Fig. 7 Proposed model depicting the functions of BnaNTT2 in cell metabolism. BnaNTT2 transports cytosolic ATP into plastid and exchanges ADP into cytoplasm. Overexpression of *BnaC08.NTT2* promotes the transportation of more ATP into plastid and enhances starch and fatty acid synthesis. Enhanced metabolism in plastid promotes the glycolysis in cytoplasm. Meanwhile, *WRI1* is a key transcription factor for fatty acid synthesis, playing a "push" role in fatty acid de novo synthesis. Loss function of *BnaNTT2* decreases the transportation of ATP into plastid, leading to decreased fatty acid and chloroplast membrane lipid biosynthesis, which could result in abnormal thylakoid structure. AGPase, ADP-glucose pyrophosphorylase; ACCase, acetyl-CoA carboxylase

plastid are used to compose membrane lipids such as MGDG, DGDG, and PG which determine the thylakoid structure and photosynthesis efficiency (Fig. 7). BnaNTT2 enhances the supplying of ATP and primary metabolites into plastid to improve FA synthesis. Enhanced glycolysis is required to release more energy to maintain the action of other organelles in cytoplasm, and this process possibly induces *WRI1* activity (Zhai et al. 2021; Cernac and Benning 2004). The "push" role of *WRI1* will improve FA biosynthesis (Vanhercke et al. 2013). This feedback mechanism of glycolysis improves the *WRI1* activity to accelerate FA biosynthesis, which needs more metabolites and ATP produced from glycolysis (Fig. 7). Thus, BnaNTT2 plays multiple and key roles in sustaining primary metabolism, lipid synthesis, and plant growth in *B. napus*.

Acknowledgements We are grateful to the Open Sharing Platform at Huazhong Agricultural University for the help with TEM and confocal laser scanning scope in this research.

Author contribution S.T. and L.G. designed this study. Y.H., H.X., X.L., R.F., Q.L., and Z.O. performed the experiments. Y.H. analyzed the data. Y.H. wrote the manuscript. S.T., L.G., S.L., X.L., and X.Y. revised the manuscript.

Funding The work was supported by grant from the National Natural Science Foundation of China (31900908, 31871658).

Data availability All data and materials generated or analyzed during this study are included in this article and its supplementary information files.

Not applicable.

Declarations

Consent to participate The authors are consented to participate.

Consent for publication The authors are consented for publication.

Conflict of interest The authors declare no competing interests.

References

Andersson M, Turesson H, Arrivault S, Zhang Y, Falt AS, Fernie AR, Hofvander P (2018) Inhibition of plastid PPase and NTT leads to major changes in starch and tuber formation in potato. J Exp Bot 69(8):1913–1924. https://doi.org/10.1093/jxb/ery051

Baud S, Mendoza MS, To A, Harscoet E, Lepiniec L, Dubreucq B (2007) *WRINKLED1* specifies the regulatory action of *LEAFY COTYLEDON2* towards fatty acid metabolism during seed maturation in Arabidopsis. Plant J 50(5):825–838. https://doi.org/10.1111/j.1365-313X.2007.03092.x

Baud S, WuillÃme S, To A, Rochat C, Lepiniec LC (2009) Role of *WRINKLED1* in the transcriptional regulation of glycolytic and fatty acid biosynthetic genes in Arabidopsis. Plant J 60(6):933–947. https://doi.org/10.1111/j.1365-313X.2009.04011.x

Block MA (2018) Isolation of inner and outer membranes of the chloroplast envelope from Spinach and Pea. Methods Mol Biol 1829:137–144. https://doi.org/10.1007/978-1-4939-8654-5_9

Bourgis F, Kilaru A, Cao X, Ngando-Ebongue GF, Drira N, Ohlrogge JB, Arondel V (2011) Comparative transcriptome and metabolite analysis of oil palm and date palm mesocarp that differ dramatically in carbon partitioning. P Natl Acad Sci USA 108(30):12527–12532. https://doi.org/10.1073/pnas.1106502108

Cai Y, Goodman JM, Pyc M, Mullen RT, Dyer JM, Chapman KD (2015) Arabidopsis SEIPIN proteins modulate triacylglycerol accumulation and influence lipid droplet proliferation. Plant Cell 27(9):2616–2636. https://doi.org/10.1105/tpc.15.00588

Cernac A, Benning C (2004) *WRINKLED1* encodes an AP2/EREB domain protein involved in the control of storage compound biosynthesis in Arabidopsis. Plant J 40(4):575–585. https://doi.org/10.1111/j.1365-313X.2004.02235.x

Chow PS, Landhausser SM (2004) A method for routine measurements of total sugar and starch content in woody plant tissues. Tree Physiol 24(10):1129–1136. https://doi.org/10.1093/treephys/24.10.1129

Dai C, Li Y, Li L, Du Z, Lu S (2020) An efficient agrobacterium-mediated transformation method using hypocotyl as explants for *Brassica napus*. Mol Breeding 40(10):96. https://doi.org/10.1007/s11032-020-01174-0

Fan K, Rawsthorne S (1994) Starch and fatty acid synthesis in plastids from developing embryos of oilseed rape (Brassica napus L.). Plant J 6(6):795–805. https://doi.org/10.1046/j.1365-313X.1994.6060795.x

Flugge UI, Hausler RE, Ludewig F, Gierth M (2011) The role of transporters in supplying energy to plant plastids. J Exp Bot 62(7):2381–2392. https://doi.org/10.1093/jxb/erq361

Geigenberger P, Stamme C, Tjaden J, Schulz A, Quick PW, Betsche T, Kersting HJ, Neuhaus HE (2001) Tuber physiology and properties of starch from tubers of transgenic potato plants with altered plastidic adenylate transporter activity. Plant Physiol 125(4):1667–1678. https://doi.org/10.1104/pp.125.4.1667

Guo L, Ma F, Wei F, Fanella B, Allen DK, Wang X (2014) Cytosolic phosphorylating glyceraldehyde-3-phosphate dehydrogenases affect Arabidopsis cellular metabolism and promote seed oil accumulation. Plant Cell 26(7):3023–3035. https://doi.org/10.1105/tpc.114.126946

Haferkamp I, Hackstein JH, Voncken FG, Schmit G, Tjaden J (2002) Functional integration of mitochondrial and hydrogenosomal ADP/ATP carriers in the *Escherichia coli* membrane reveals different biochemical characteristics for plants, mammals and anaerobic chytrids. Eur J

Biochem 269(13):3172–3181. https://doi.org/10.1046/j.1432-1033.2002.02991.x

Hattori M, Hibbs RE, Gouaux E (2012) A fluorescence-detection size-exclusion chromatography-based thermostability assay for membrane protein precrystallization screening. Structure 20(8):1293–1299. https://doi.org/10.1016/j.str.2012.06.009

Hong Y, Xia H, Li X, Fan R, Li Q, Ouyang Z, Tang S, Guo L (2022) *Brassica napus BnaNTT1* modulates ATP homeostasis in plastids to sustain metabolism and growth. Cell Rep 40(2):111060. https://doi.org/10.1016/j.celrep.2022.111060

Hong Y, Yuan S, Sun L, Wang X, Hong Y (2018) Cytidinediphosphate-diacylglycerol synthase 5 is required for phospholipid homeostasis and is negatively involved in hyperosmotic stress tolerance. Plant J 94(6):1038–1050. https://doi.org/10.1111/tpj.13916

Kong Q, Ma W (2018) *WRINKLED1* as a novel 14–3-3 client: function of 14–3-3 proteins in plant lipid metabolism. Plant Signal Behav 13(8):e1482176. https://doi.org/10.1080/15592324.2018.1482176

Kong Q, Yang Y, Guo L, Yuan L, Ma W (2020) Molecular basis of plant oil biosynthesis: insights gained from studying the *WRINKLED1* transcription factor. Front Plant Sci 11:24. https://doi.org/10.3389/fpls.2020.00024

Kusumi K, Yara A, Mitsui N, Tozawa Y, Iba K (2004) Characterization of a rice nuclear-encoded plastid RNA polymerase gene *OsRpoTp*. Plant Cell Physiol 45(9):1194–1201. https://doi.org/10.1093/pcp/pch133

Lee EJ, Oh M, Hwang JU, Li-Beisson Y, Nishida I, Lee Y (2017) Seed-specific overexpression of the pyruvate transporter *BASS2* increases oil content in Arabidopsis seeds. Front Plant Sci 8(194):1–10. https://doi.org/10.3389/fpls.2017.00194

Li-Beisson Y, Shorrosh B, Beisson F, Andersson MX, Arondel V, Bates PD, Baud S, Bird D, Debono A, Durrett TP, Franke RB, Graham IA, Katayama K, Kelly AA, Larson T, Markham JE, Miquel M, Molina I, Nishida I, Rowland O, Samuels L, Schmid KM, Wada H, Welti R, Xu C, Zallot R, Ohlrogge J (2013) Acyl-Lipid Metabolism. Arabidopsis Book 11:e0161. https://doi.org/10.1199/tab.0161

Li D, Guo Y, Zhang D, He S, Gong J, Ma H, Gao X, Wang Z, Jiang L, Dun X, Hu S, Chen M (2020) Melatonin represses oil and anthocyanin accumulation in seeds. Plant Physiol 183(3):898–914. https://doi.org/10.1104/pp.20.00117

Li N, Gugel IL, Giavalisco P, Zeisler V, Schreiber L, Soll J, Philippar K (2015) FAX1, a novel membrane protein mediating plastid fatty acid export. PLoS Biol 13(2):e1002053. https://doi.org/10.1371/journal.pbio.1002053

Linka N, Hurka H, Lang BF, Burger G, Winkler HH, Stamme C, Urbany C, Seil I, Kusch J, Neuhaus HE (2003) Phylogenetic relationships of non-mitochondrial nucleotide transport proteins in bacteria and eukaryotes. Gene 306:27–35. https://doi.org/10.1016/s0378-1119(03)00429-3

Lu S, Bahn SC, Qu G, Qin H, Hong Y, Xu Q, Zhou Y, Hong Y, Wang X (2013) Increased expression of phospholipase Dα1 in guard cells decreases water loss with improved seed production under drought in *Brassica napus*. Plant Biotechnol J 11(3):380–389. https://doi.org/10.1111/pbi.12028

Lu S, Liu H, Jin C, Li Q, Guo L (2019) An efficient and comprehensive plant glycerolipids analysis approach based on high-performance liquid chromatography–quadrupole time-of-flight mass spectrometer. Plant Direct 3(11):1–13. https://doi.org/10.1002/pld3.183

Lyu J, Wang Y, Liu L, Wang C, Ren Y, Peng C, Liu F, Wang Y, Niu M, Wang D, Zheng M, Zhou K, Zhao S, Wu F, Wang H, Wan J (2017) A putative plastidial adenine nucleotide transporter, BRITTLE1-3, plays an essential role in regulating chloroplast development in rice (Oryza sativa L.). J Plant Biol 60(5):493–505. https://doi.org/10.1007/s12374-017-0063-6

Möhlmann T, Neuhaus RSE (1994) Interaction between fatty-acid and starch synthesis in isolated amyloplasts from cauliflower floral buds. Planta 194(4):492–497. https://doi.org/10.1007/BF00714461

Maeo K, Tokuda T, Ayame A, Mitsui N, Kawai T, Tsukagoshi H, Ishiguro S, Nakamura K (2009) An AP2-type transcription factor, *WRINKLED1*, of *Arabidopsis thaliana* binds to the AW-box sequence conserved among proximal upstream regions of genes involved in fatty acid synthesis. Plant J 60(3):476–487. https://doi.org/10.1111/j.1365-313X.2009.03967.x

Mohlmann T, Tjaden J, Schwoppe C, Winkler HH, Kampfenkel K, Neuhaus HE (1998) Occurrence of two plastidic ATP/ADP transporters in Arabidopsis thaliana L.–molecular characterisation and comparative structural analysis of similar ATP/ADP translocators from plastids and Rickettsia prowazekii. Eur J Biochem 252(3):353–359. https://doi.org/10.1046/j.1432-1327.1998.2520353.x

Moreira D, Le Guyader H, Philippe H (2000) The origin of red algae and the evolution of chloroplasts. Nature 405(6782):69–72. https://doi.org/10.1038/35011054

Mullet JE (1993) Dynamic regulation of chloroplast transcription. Plant Physiol 103(2):309–313. https://doi.org/10.1104/pp.103.2.309

Neuhaus H, Maass U (1996) Unidirectional transport of orthophosphate across the envelope of isolated cauliflower-bud amyloplasts. Planta 198(4):542–548. https://doi.org/10.1007/BF00262640

Neuhaus HE, Emes MJ (2000) Nonphotosynthetic metabolism in plastids. Annu Rev Plant Physiol Plant Mol Biol 51:111–140. https://doi.org/10.1146/annurev.arplant.51.1.111

Qi Q, Kleppinger-Sparace KF, Sparace SA (1994) The role of the triose-phosphate shuttle and glycolytic intermediates in fatty-acid and glycerolipid biosynthesis in pea root plastids. Planta 194(2):193–199. https://doi.org/10.1007/bf01101678

Reiser J, Linka N, Lemke L, Jeblick W, Neuhaus HE (2004) Molecular physiological analysis of the two plastidic ATP/ADP transporters from Arabidopsis. Plant Physiol 136(3):3524–3536. https://doi.org/10.1104/pp.104.049502

Reynolds KB, Taylor MC, Zhou XR, Vanhercke T, Wood CC, Blanchard CL, Singh SP, Petrie JR (2015) Metabolic engineering of medium-chain fatty acid biosynthesis in *Nicotiana benthamiana* plant leaf lipids. Front Plant Sci 6:164. https://doi.org/10.3389/fpls.2015.00164

Rieder B, Neuhaus HE (2011) Identification of an Arabidopsis plasma membrane-located ATP transporter important for

anther development. Plant Cell 23(5):1932–1944. https://doi.org/10.1105/tpc.111.084574

Roux SJ, Steinebrunner I (2007) Extracellular ATP: an unexpected role as a signaler in plants. Trends Plant Sci 12(11):522–527. https://doi.org/10.1016/j.tplants.2007.09.003

Sanjaya DTP, Weise SE, Benning C (2011) Increasing the energy density of vegetative tissues by diverting carbon from starch to oil biosynthesis in transgenic Arabidopsis. Plant Biotechnol J 9(8):874–883. https://doi.org/10.1111/j.1467-7652.2011.00599.x

Schmitz-Esser S, Linka N, Collingro A, Beier CL, Neuhaus HE, Wagner M, Horn M (2004) ATP/ADP translocases: a common feature of obligate intracellular amoebal symbionts related to Chlamydiae and Rickettsiae. J Bacteriol 186(3):683–691. https://doi.org/10.1128/JB.186.3.683-691.2004

Slabas AR, Fawcett T (1992) The biochemistry and molecular biology of plant lipid biosynthesis. Plant Mol Biol 19(1):169–191. https://doi.org/10.1007/BF00015613

Song CJ, Steinebrunner I, Wang X, Stout SC, Roux SJ (2006) Extracellular ATP induces the accumulation of superoxide via NADPH oxidases in Arabidopsis. Plant Physiol 140(4):1222–1232. https://doi.org/10.1104/pp.105.073072

Steinebrunner I, Wu J, Sun Y, Corbett A, Roux SJ (2003) Disruption of apyrases inhibits pollen germination in Arabidopsis. Plant Physiol 131(4):1638–1647. https://doi.org/10.1104/pp.102.014308

Tang T, Yu X, Yang H, Gao Q, Ji H, Wang Y, Yan G, Peng Y, Luo H, Liu K, Li X, Ma C, Kang C, Dai C (2018) Development and validation of an effective CRISPR/Cas9 vector for efficiently isolating positive transformants and transgene-free mutants in a wide range of plant species. Front Plant Sci 9:1533. https://doi.org/10.3389/fpls.2018.01533

Tang W, Brady SR, Sun Y, Muday GK, Roux SJ (2003) Extracellular ATP inhibits root gravitropism at concentrations that inhibit polar auxin transport. Plant Physiol 131(1):147–154. https://doi.org/10.1104/pp.013672

Tjaden J, Schwoppe C, Mohlmann T, Quick PW, Neuhaus HE (1998) Expression of a plastidic ATP/ADP transporter gene in Escherichia coli leads to a functional adenine nucleotide transport system in the bacterial cytoplasmic membrane. J Biol Chem 273(16):9630–9636. https://doi.org/10.1074/jbc.273.16.9630

To A, Joubes J, Barthole G, Lecureuil A, Scagnelli A, Jasinski S, Lepiniec L, Baud S (2012) *WRINKLED* transcription factors orchestrate tissue-specific regulation of fatty acid biosynthesis in Arabidopsis. Plant Cell 24(12):5007–5023. https://doi.org/10.1105/tpc.112.106120

Trentmann O, Jung B, Neuhaus HE, Haferkamp I (2008) Non-mitochondrial ATP/ADP transporters accept phosphate as third substrate. J Biol Chem 283(52):36486–36493. https://doi.org/10.1074/jbc.M806903200

van Erp H, Kelly AA, Menard G, Eastmond PJ (2014) Multigene engineering of triacylglycerol metabolism boosts seed oil content in Arabidopsis. Plant Physiol 165(1):30–36. https://doi.org/10.1104/pp.114.236430

Vanhercke T, El Tahchy A, Shrestha P, Zhou XR, Singh SP, Petrie JR (2013) Synergistic effect of *WRI1* and *DGAT1* coexpression on triacylglycerol biosynthesis in plants. FEBS Lett 587(4):364–369. https://doi.org/10.1016/j.febslet.2012.12.018

Voon CP, Lim BL (2019) ATP translocation and chloroplast biology. Natl Sci Rev 6(6):1073–1076. https://doi.org/10.1093/nsr/nwz089

Weber AP (2004) Solute transporters as connecting elements between cytosol and plastid stroma. Curr Opin Plant Bio 7(3):247–253. https://doi.org/10.1016/j.pbi.2004.03.008

Weber APM, Linka N (2011) Connecting the plastid: transporters of the plastid envelope and their role in linking plastidial with cytosolic metabolism. Annu Rev Plant Biol 62(1):53–77. https://doi.org/10.1146/annurev-arplant-042110-103903

Welti R, Li W, Li M, Sang Y, Biesiada H, Zhou HE, Rajashekar CB, Williams TD, Wang X (2002) Profiling membrane lipids in plant stress responses. Role of phospholipase D alpha in freezing-induced lipid changes in Arabidopsis. J Biol Chem 277(35):31994–32002. https://doi.org/10.1074/jbc.M205375200

Winkler HH, Neuhaus HE (1999) Non-mitochondrial ATP transport. Trends Biochem Sci 24(2):64–68. https://doi.org/10.1016/s0968-0004(98)01334-6

Xu C, Shanklin J (2016) Triacylglycerol metabolism, function, and accumulation in plant vegetative tissues. Annu Rev Plant Biol 67:179–206. https://doi.org/10.1146/annurev-arplant-043015-111641

Zhai Z, Keereetaweep J, Liu H, Xu C, Shanklin J (2021) The role of sugar signaling in regulating plant fatty acid synthesis. Front Plant Sci 12:643843. https://doi.org/10.3389/fpls.2021.643843

Zhou Z, Dun X, Xia S, Shi D, Qin M, Yi B, Wen J, Shen J, Ma C, Tu J, Fu T (2012) *BnMs3* is required for tapetal differentiation and degradation, microspore separation, and pollen-wall biosynthesis in *Brassica napus*. J Exp Bot 63(5):2041–2058. https://doi.org/10.1093/jxb/err405